

Electronic and structural properties of dense liquid and amorphous nitrogen

Brian Boates and Stanimir A. Bonev

*Lawrence Livermore National Laboratory, Livermore, California 94551, USA and**Department of Physics, Dalhousie University, Halifax, Nova Scotia B3H 3J5, Canada*

(Received 2 March 2011; revised manuscript received 19 April 2011; published 31 May 2011)

We present first-principles calculations of the structural and electronic properties of liquid nitrogen in the pressure-temperature range of 0–200 GPa and 2000–6000 K. Upon polymerization, the liquid becomes metallic, similar to what has been reported for the higher temperature atomic fluid. An explanation of the electronic properties of the transformed liquids and the differences with the electronic properties of insulating solid cubic-gauche nitrogen is given based on the structure and bonding character of these phases. The mechanism responsible for charge transport in polymeric nitrogen systems is examined in order to understand the semiconducting nature of low-temperature amorphous nitrogen.

DOI: [10.1103/PhysRevB.83.174114](https://doi.org/10.1103/PhysRevB.83.174114)

PACS number(s): 62.50.–p, 02.70.–c, 61.20.Ja, 31.15.at

I. INTRODUCTION

The behavior of molecular solids and liquids under extreme conditions is of fundamental interest in the field of condensed matter physics and chemistry. At high pressures (P) and temperatures (T) these materials often undergo dissociation and/or polymerization transitions to new phases with interesting properties.^{1,2} In particular, polymeric nitrogen has become a subject of intense research in recent years. If metastable under ambient conditions, polymeric nitrogen could be important as a high-energy-density material. At pressures near and above 100 GPa molecular nitrogen was found to transform into a narrow-gap (~ 0.6 eV) semiconducting amorphous phase (η -N).^{3–6} Extrapolation of experimental band gap energies suggests that η -N becomes metallic above 300 GPa at room temperature.⁵ Above 2000 K at comparable pressures, nitrogen forms the insulating single-bonded cubic-gauche phase (cg-N). This phase was predicted⁷ over a decade before its experimental verification.¹ Recently, there have been many studies on the thermodynamic stability of other polymeric crystalline phases of nitrogen, with some possessing lower enthalpy than cg-N at higher pressures, although none have been observed experimentally.^{8–17}

Previous shock-wave experiments have shown that molecular liquid nitrogen undergoes a continuous transformation to a conducting atomic liquid at high P and T .^{18–20} Subsequent first-principles calculations^{21,22} also reported molecular dissociation and metallization in good agreement with experiment. In both studies, the authors emphasize the correlation between the fraction of dissociated atoms and the electrical conductivity, as it is states attributed to the dissociated atoms that begin to populate the dense liquid band gap.

At lower temperatures it was predicted that the molecular liquid undergoes a first-order phase transition to a polymeric liquid upon compression.²³ The structure of the emerging liquid continues to evolve with pressure; upon transformation, the liquid is predominantly 2-coordinated while further compression yields more 3-coordinated atoms. The band gap was found to close upon transformation to the polymeric liquid, indicating that the molecular-polymeric transition may coincide with an insulator-metal transition.²⁴

In this paper, we report the results of first-principles calculations on the structural and electronic properties of liquid nitrogen. The frequency-dependent conductivity $\sigma(\omega)$ and reflectivity $R(\omega)$ of liquid nitrogen have been calculated. The polymeric liquid is metallic in contrast to the known insulating polymeric solid cg-N. We provide an explanation for this difference based on differences in the structure and bonding of the two phases. An analogy is made between the polymeric liquid and the low-temperature semiconducting amorphous solid based on compelling similarities in their structure. The mechanism responsible for electronic transport in polymeric nitrogen is presented and used to explain the differences in the electronic properties of the two disordered polymeric phases.

II. COMPUTATIONAL METHOD**A. First-principles molecular dynamics**

First-principles molecular dynamics (FPMD) simulations of nitrogen have been performed for pressures up to 200 GPa and temperatures up to 6000 K using finite-temperature density functional theory (DFT)²⁵ within the Perdew-Burke-Ernzerhof generalized gradient approximation (PBE-GGA)²⁶ as implemented in VASP.²⁷ The FPMD simulations were carried out in the canonical (NVT) ensemble using Born-Oppenheimer dynamics and a Nosé-Hoover thermostat. Simulations were equilibrated within 1–2 ps and continued for over 10 ps using 0.75 and 0.50 fs ionic time steps. Simulations were performed with 64- and 128-atom supercells, a 5-electron projector augmented wave (PAW) pseudopotential with a 1.50 bohr core radius, and a 500 eV plane-wave cutoff. Changes in E , P , and the structure were negligible when checked using a PAW pseudopotential with a 1.10 bohr core radius with a 944.5 eV plane-wave cutoff.

Further convergence studies of \mathbf{k} -point sampling and finite-size effects were carried out over a wide range of P - T conditions: before and after polymerization and dissociation, as well as at the highest pressures considered. These included (i) FPMD simulations with 64-atom supercells and a $2 \times 2 \times 2$ \mathbf{k} -point grid; and (ii) static calculations with a $2 \times 2 \times 2$

$4 \times 4 \times 4$ \mathbf{k} -point grid on 128-atom FPMD configurations. In all cases, changes in E , P , and the structure were well within the error bars.

To validate our methods we have calculated the P - V equation of state (EOS) of cg-N at finite temperature in good agreement with experimental data^{28,29} which was shown in our previous work.²³ Vibrational frequencies in our simulated molecular fluid also compare well with experimental results³⁰ near 50 GPa and 2000 K. Furthermore, our simulations suggest the onset of molecular dissociation above 30 GPa at 6000 K in excellent agreement with previous experimental²⁰ and theoretical work.²²

B. Electronic properties

The electronic conductivity was evaluated for several densities along the 2000, 3000, and 6000 K isotherms. At each density considered, the conductivity was averaged over 10–30 well-spaced configurations from a 64-atom FPMD trajectory. The occupation of the orbitals was determined based on a Fermi-Dirac distribution with an electronic temperature equal to the ionic temperature. For these calculations we have used a 5-electron PAW pseudopotential with a 1.11 bohr core radius, a 40 hartree plane-wave cutoff within PBE-GGA DFT in ABINIT,^{31,32} and a $4 \times 4 \times 4$ \mathbf{k} -point grid. The real part of the frequency-dependent conductivity was evaluated using the Kubo-Greenwood formalism:^{33,34}

$$\sigma_1(\omega) = \frac{2\pi e^2 \hbar^2}{3m^2 \omega \Omega} \sum_{\mathbf{k}} W(\mathbf{k}) \sum_{j=1}^N \sum_{i=1}^N \sum_{\alpha=1}^3 [F(\epsilon_{i,\mathbf{k}}) - F(\epsilon_{j,\mathbf{k}})] \times |\langle \Psi_{j,\mathbf{k}} | \nabla_{\alpha} | \Psi_{i,\mathbf{k}} \rangle|^2 \delta(\epsilon_{i,\mathbf{k}} - \epsilon_{j,\mathbf{k}} - \hbar\omega), \quad (1)$$

where m and e are the mass and charge of an electron, Ω is the cell volume, α is an index over spatial directions, and $F(\epsilon_{i,\mathbf{k}})$ represents the occupation of the i th eigenvalue at \mathbf{k} point \mathbf{k} . The zero-frequency limit of this expression yields the direct current (DC) conductivity σ_{DC} . The imaginary part of the frequency-dependent conductivity is given by the Kramers-Krönig transform:

$$\sigma_2(\omega) = -\frac{2}{\pi} P \int_0^{\infty} \frac{\sigma(v)\omega}{(v^2 - \omega^2)} dv, \quad (2)$$

where the principal value of the integral is given by P . The complex dielectric function ϵ , index of refraction n , coefficient of extinction k , and reflectivity R can be obtained using the complex conductivity:

$$\epsilon_1(\omega) = 1 - \frac{4\pi}{\omega} \sigma_2(\omega), \quad \epsilon_2(\omega) = \frac{4\pi}{\omega} \sigma_1(\omega), \quad (3)$$

$$\epsilon(\omega) = \epsilon_1(\omega) + i\epsilon_2(\omega) = [n(\omega) + ik(\omega)]^2, \quad (4)$$

$$R(\omega) = \frac{[1 - n(\omega)]^2 + k^2(\omega)}{[1 + n(\omega)]^2 + k^2(\omega)}. \quad (5)$$

III. RESULTS

A. Electronic properties

The electronic density of states (DOS) of liquid nitrogen is shown in Fig. 1 for several densities along the 3000 K isotherm. At low pressure the liquid is molecular and insulating

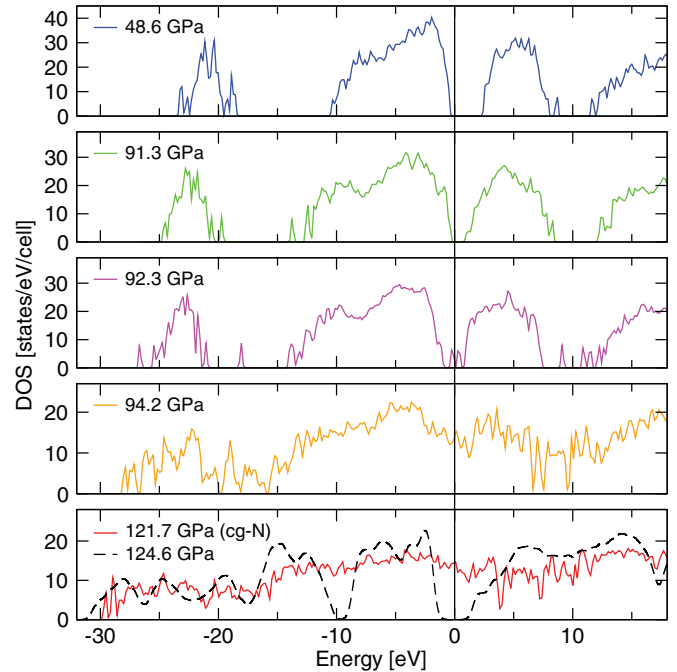


FIG. 1. (Color online) Electronic density of states of liquid nitrogen at 3000 K and insulating cg-N at 2000 K. States begin to populate the band gap as the molecular liquid transforms into the polymeric liquid phase, before closing the gap entirely over a very small pressure range. At 3000 K the liquid-liquid transition occurs at 92 GPa.

with a GGA band gap of approximately 2 eV. The DOS at 2000 K of the known single-bonded insulating solid phase, cg-N, is also shown for comparison. Upon compression the DOS remains relatively unchanged until approaching the polymerization transition. As the triple-bonded molecules begin to destabilize, new polymeric compounds are formed and the band gap closes rapidly with pressure. Thus, the liquid polymerization transition coincides with an insulator-metal transition as previously reported by Donadio *et al.*²⁴ The results shown in Fig. 1 are in good quantitative agreement with the liquid DOS at 90 and 120 GPa, reported in Ref. 24.

Figure 2 shows the frequency-dependent conductivity of liquid nitrogen along the 3000 K isotherm. The low-density molecular liquid possesses two distinct peaks which gradually disappear with increasing pressure. Most notable is the jump in DC conductivity upon reaching the liquid phase boundary near 92 GPa. The inset shows the DC conductivity as a function of pressure along the 3000 and 6000 K isotherms. The DC conductivity is zero at low pressures as the fluid is purely molecular. At the 3000 K liquid-liquid phase boundary, the DC conductivity sharply increases to a nearly constant value of 3000 $(\Omega \cdot \text{cm})^{-1}$. A similar increase is also found in σ_{DC} along the 6000 K isotherm, consistent with previous calculations of dissociating liquid nitrogen along the 5000 K isotherm.²² Note the gradual increase in the conductivity as the molecules dissociate compared to the discontinuous increase when they undergo polymerization. This is a result of the gradual nature of the high- T dissociation transition of nitrogen molecules, whereas the lower T polymerization is first order.

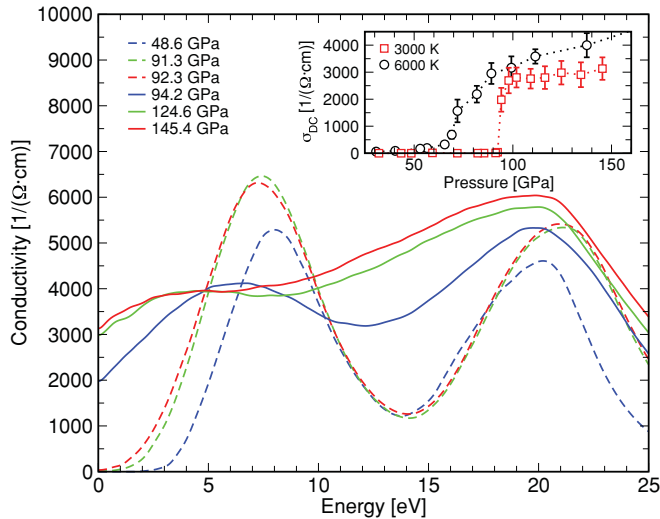


FIG. 2. (Color online) Frequency-dependent conductivity of liquid nitrogen along the 3000 K isotherm. (Inset) DC conductivity as a function of pressure along the 3000 (red) and 6000 K (black) isotherms.

The frequency-dependent reflectivity along the 3000 K isotherm is shown in Fig. 3. The reflectivity curves show a progression similar to what we find in the computed conductivities. As the reflectivity is a common experimental observable, we provide its pressure dependence at 3000 and 6000 K for wavelengths of 532 and 1064 nm. The reflectivities at these wavelengths increase sharply at the 3000 K polymerization phase boundary and plateau to a value near 0.70. For comparison, they are also shown at 6000 K where they increase gradually with pressure before plateauing to comparable values. Measurement of the conductivity and reflectivity may prove useful in the experimental detection

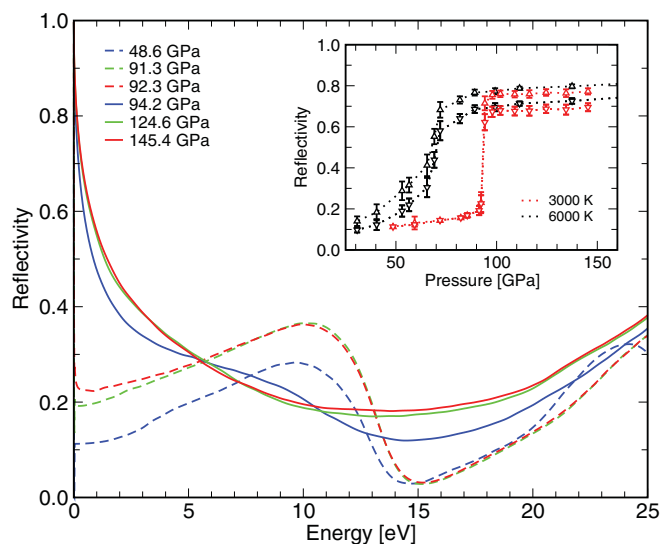


FIG. 3. (Color online) Frequency-dependent reflectivity of liquid nitrogen along the 3000 K isotherm. (Inset) Reflectivity at 532 (downward triangles) and 1064 nm (upward triangles) as a function of pressure for 3000 (red) and 6000 K (black) isotherms.

of the polymeric fluid and in future measurements of the high-pressure melting curve.

B. Relation to structural properties

At low pressure, the insulating nature of molecular liquid nitrogen can simply be explained by the electrons being strongly localized within the triple bond. At very high temperatures, the molecular bonds destabilize upon compression and begin to dissociate into a metallic atomic phase. The metallization in this regime has been previously explained^{21,22} in terms of dopant dissociated atoms filling the band gap. However, we note that the Goldhammer-Herzfeld (GH) criterion for metallization in atomic N is not satisfied until 223 GPa, indicating that the mechanism responsible for conductivity may be more complex. At lower temperatures, the breaking of molecules leads to the formation of covalently bonded polymeric compounds rather than dissociated atoms. Despite the covalent bonding, the polymeric liquid is conducting. Moreover, the known polymeric cg-N solid is an insulator, while the low- T amorphous η -N phase is semiconducting. Thus, there are significant differences in the electronic structure of the different polymeric phases.

In order to understand the origin of these differences, we relate the observed electronic behavior to the structure of the polymeric phases. We consider the atomic coordination, defined as the number of atoms surrounding a given ion within a selected cutoff distance. As covalent bonds are within the first peak of the pair correlation function $g(r)$, we have chosen our cutoff as the first minimum of $g(r)$. Figure 4 (top) shows the DC conductivity of liquid nitrogen at 2000, 3000, and 6000 K. Amorphous and chainlike solids obtained through freezing of the high- P liquid at 2000 K are also shown. The fraction of 2-coordinated nitrogen atoms in each phase is given for direct comparison in Fig. 4 (bottom).

The DC conductivity is zero for the low- P molecular liquid at 2000, 3000, and 6000 K, which coincides with the purely 1-coordinated nature of the atoms or, equivalently, triple bonding. Upon compression, the liquid transforms into the polymeric phase at similar pressures for both 2000 and 3000 K. This leads to an increase in the fraction of 2-coordinated atoms in the system to approximately 75% and 60%, respectively. The increase in 2-coordinated atoms is accompanied by a qualitatively identical increase in σ_{DC} to approximately $3000 (\Omega\cdot\text{cm})^{-1}$, which remains relatively constant under further compression. The plateauing of σ_{DC} with pressure is mirrored in the near-constant fraction of 2-coordinated atoms and can also be explained by the constant nearest-neighbor bond length of 1.27 Å at these pressures.

At 6000 K the liquid undergoes a continuous molecular dissociation; however, we find that the resulting dissociated high- T fluid is also predominantly 2-coordinated. The important structural difference between the atomic and polymeric fluids is therefore the dynamic stability of 2-coordinated nitrogen compounds, not simply their static presence. Thus, the conductivity in the atomic liquid can also be attributed to the presence of short-lived 2-coordinated compounds, similar to the polymeric case. We emphasize that the finite σ_{DC} of the 6000 K fluid is not a temperature (ionization) effect. When Eq. (1) is evaluated using atomic configurations

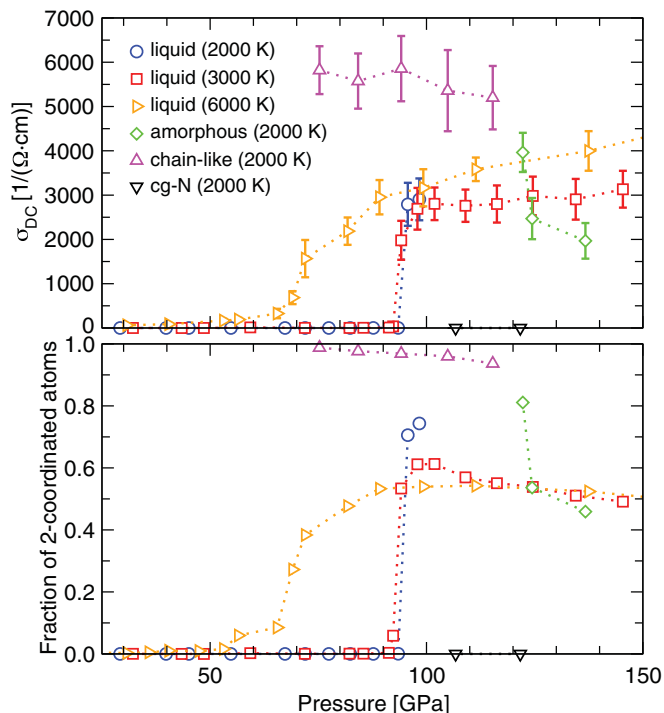


FIG. 4. (Color online) (Top) DC conductivity as a function of pressure for the 2000 K liquid (circles), 3000 K liquid (squares), 6000 K liquid (right triangles), 2000 K chainlike solid (upward triangles), 2000 K amorphous solid (diamonds), and cg-N at 2000 K (downward triangles). (Bottom) Fraction of 2-coordinated atoms in each corresponding phase.

from a 6000 K simulation but with a Fermi-Dirac smearing of only 300 K, σ_{DC} remains essentially unchanged.

If one considers the aforementioned chainlike and amorphous solid phases obtained through FPMD freezing of the 2000 K liquid, one also finds a strong correlation between the 2-coordinated fraction and σ_{DC} . Almost all atoms in the chainlike phase are 2-coordinated resulting in a heightened DC conductivity. The high- T amorphous solid shares similar structural characteristics with the polymeric liquid, but possesses a slightly lowered conductivity, which may provide insight into the semiconducting nature of the η -N phase.

Lastly, entirely single-bonded (3-coordinated) cg-N is shown to illustrate how polymeric nitrogen without 2-coordinated atoms results in zero DC conductivity. Thus, phases that are purely 1-coordinated (molecular) and 3-coordinated (cg-N) exhibit no DC conductivity. The DC conductivity below 200 GPa is only nonzero when 2-coordinated atoms are present and the value of σ_{DC} is strongly correlated to the fraction of such atoms. Conductivity resulting from electrons traveling along 2-coordinated nitrogen chainlike compounds is analogous to what is known for carbon hydrides such as trans-polyacetylene and is discussed in the following section.

C. Amorphous nitrogen

Conducting polymers have been a subject of intense research for several years.³⁵ The prototypical example of a one-dimensional (1D) conducting polymer is trans-polyacetylene

(trans-PA). The idealized structure of trans-PA can be described as a chain of equally spaced CH groups. In this configuration trans-PA would be a 1D metal, as each carbon atom would supply one electron to a subsequently half filled π band. However, at low temperatures trans-PA undergoes a Peierls distortion, leading to a chain of alternating single- and double-bonded CH groups. This opens a gap at the Fermi level, making trans-PA a semiconductor rather than a metal. The resulting experimental³⁶ (theoretical³⁷) band gap and bond length alternation (BLA) are 1.5 eV (1.3 eV) and 0.08 Å (0.074 Å), respectively. The BLA is a common parameter used to describe Peierls distortions and is simply the difference in lengths of the bonds between neighboring atoms.³⁶ To describe the electronic properties of trans-PA, the so-called SSH Hamiltonian was written, assuming that the local electronic density can be coupled to the length of the covalent bonds between carbon atoms along the chain and that the electronic structure of the π bands can be described within a tight-binding approximation as

$$4t_{n+1,n} = t_0 - \alpha(u_{n+1} - u_n), \quad (6)$$

$$H_{SSH} = \sum_{n,\sigma} -t_{n+1,n}(c_{n+1,\sigma}^\dagger c_{n,\sigma} + c_{n,\sigma}^\dagger c_{n+1,\sigma}) + \sum_n \left[\frac{p_n^2}{2m} + \frac{1}{2} K_n (u_{n+1} - u_n)^2 \right]. \quad (7)$$

Here $t_{n+1,n}$ is the electron hopping integral to first order from the n th to the n th + 1 CH group, t_0 is the hopping integral for the equidistant chain, α is the electron-phonon coupling constant, u_n is the displacement of the n th CH group along the axis of the chain from equilibrium, $c_{n,\sigma}^\dagger$ and $c_{n,\sigma}$ are the creation and annihilation operators for π electrons on the n th CH group, p_n are the nuclear momenta, m is the atomic mass of carbon, and K_n is an effective spring constant. The second sum in (7) describes the kinetic energy of the ions as well as the potential energy arising from the displacement of CH groups along the chain. In (6) it is assumed that the effects of a Peierls distortion are sufficiently small and can be approximated linearly.

We now argue that the chains of nitrogen atoms observed in the polymeric liquid and amorphous phases are both structurally and electronically analogous to trans-PA, where the CH groups are replaced by nitrogen atoms. Electronically, this means that the hydrogen atoms are replaced by lone electron pairs in the case of nitrogen. Should this analogy hold, one should observe similar Peierls-like distortions in an idealized chain of nitrogen atoms. This effect can be captured using hybrid exchange functional techniques, as has been done for trans-PA.³⁷ To illustrate it for chainlike nitrogen compounds, we have performed hybrid Hartree-Fock (HF) and PBE-GGA exchange calculations on a prototypical 2-atom chain monomer found in both polymeric liquid and amorphous nitrogen. For these, a fixed cell with periodic boundary conditions of size $a = 10$ Å in directions perpendicular to the chain and $c = 1.90$ Å parallel to the chain was used. The value of 10 Å is sufficient to avoid interaction with periodic replicas. For c , which is responsible for the compression of the chain length, the range from 1.70 to 2.20 Å was initially considered. The value of 1.90 Å was chosen for this study

as it gives bond lengths comparable to the dense liquid and amorphous phases; a different choice of c , however, does not lead to qualitative differences.

It is interesting to note that the magnitude of the Peierls distortion varies for different choices of c . Specifically, the size of the distortion decreases for smaller c (i.e., as the chain length is compressed). In turn, the electronic band gap decreases too, which is consistent with measurements suggesting metalization of semiconducting amorphous nitrogen upon further compression.⁵ In terms of the SSH Hamiltonian description presented above, compression increases the effective spring constant K_n , leading to a larger energy penalty [the last term in (7) with respect to chain distortions].

Structural relaxations with a hybrid functional lead to large Peierls distortions, giving values for BLA as high as 0.068 Å, compared to 0.005 Å when not including any HF exchange. The prescribed amount of HF (exact) exchange to incorporate into a DFT calculation using the PBE0 functional is 25%, based on a comparison of atomization energies computed using fourth-order Moller-Plesset perturbation theory with the G1 test set.³⁸ However, small changes in the amount of mixing leads to large quantitative differences in the BLA and the band gap of our system.

Figure 5 shows results for our model system when using different fractions of HF mixing. Figure 5(a) illustrates how the size of the Peierls distortion is strongly dependent on the amount of exact exchange, as expected. Furthermore, Fig. 5(b) shows the band gap resulting from each structural relaxation. It is clear that the use of HF exchange enhances the Peierls

distortion, which opens the band gap. The band gap of the hybrid-distorted chains were calculated using the respective amount of HF exchange as well as with regular PBE. The band gap of the PBE optimized chain was also calculated with various amounts of hybrid mixing. Figure 5(c) shows the electronic band structure of optimized nitrogen chains using both PBE and PBE0 (25% HF) functionals. The effect of using hybrid functionals is twofold: (i) They lead to larger Peierls distortion, thus resulting in the opening of a band gap regardless of whether the band gap calculations are carried out with PBE or hybrid exchange; and (ii) band gaps calculated with HF mixing are of course larger than those calculated with PBE on the same structure.

The band structures of Peierls-distorted chains of nitrogen atoms were previously investigated theoretically in the work of Pohl *et al.*³⁹ They find a Peierls-like distortion using a local-density approximation (LDA) exchange-correlation functional, which we could not reproduce in this work. However, the band structures they report for the distorted chain are similar to what we show in Fig. 5(c). The notable difference between the electronic bands in polymeric nitrogen and aforementioned trans-PA is the presence of a relatively flat band located just below the Fermi level. This is attributed to the lone pairs in the nitrogen system compared to the CH σ bonds in trans-PA. It is important to note that although near the Fermi level, this band likely does not participate in electrical conductivity as the electrons are localized and have a large effective mass. It is also found to drop significantly in energy when calculated using hybrid functionals.

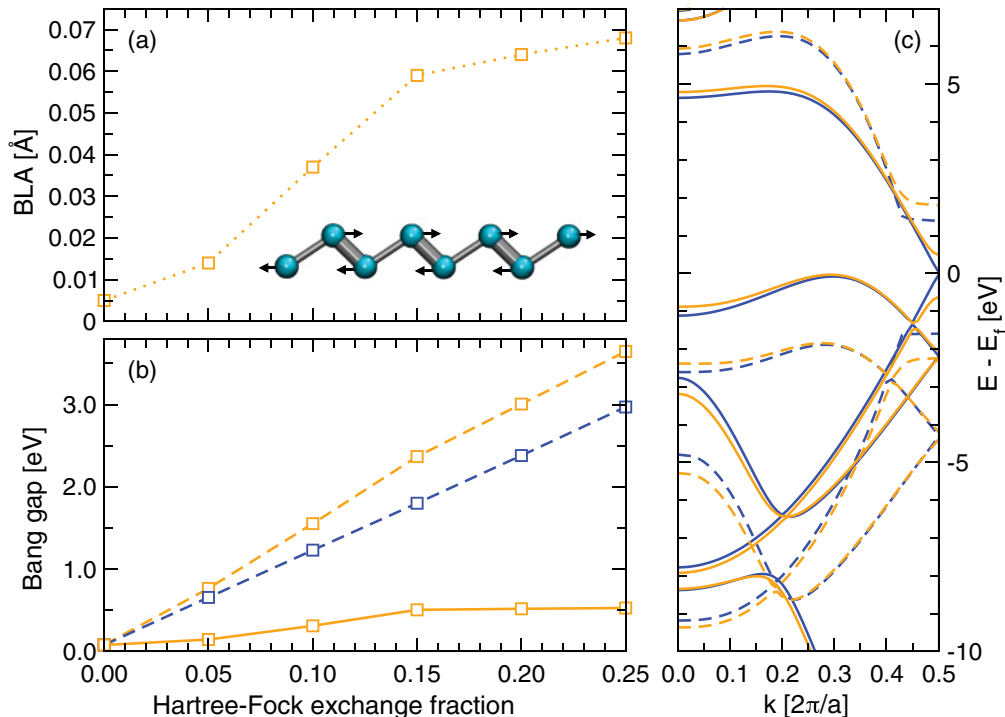


FIG. 5. (Color online) (a) Bond length alternation (BLA) of a single nitrogen chain with respect to the amount of Hartree-Fock exchange mixing (as described in the text). (b) and (c) Resulting band gaps and electronic band structures of Peierls-distorted chains using hybrid and regular PBE functionals. In both (b) and (c), calculations using a PBE (hybrid) functional for structural optimizations are shown in blue (orange); calculations of electronic properties using a PBE (hybrid) functional are given by solid (dashed) lines. A visualization of the Peierls-distorted nitrogen chain is shown in (a).

Our thesis is that similar to trans-PA the conducting behavior along chains of nitrogen atoms can be described by (7), and that the polymeric liquid and amorphous solid are characterized by these types of chainlike compounds. Thus, we propose that the polymeric liquid metal is a high-temperature manifestation of the low- T semiconducting amorphous η -N. In the polymeric liquid the Peierls distortions along the chains become negligible in comparison with the large ionic motion induced by the high temperatures. However, at lower temperatures, Peierls effects play a significant role in the electronic properties and lead to the semiconducting state of η -N. At sufficiently high density these effects are expected to diminish, as discussed earlier, and the system should metallize. The GH criterion for metallization can be used to provide an upper bound on the density at which one should expect metallization to occur due to ionization of the electrons⁴⁰ based on the gas phase polarizability. The GH densities for molecular and atomic nitrogen correspond to pressures at 300 K of approximately 509 and 223 GPa, respectively. These pressures were obtained by fitting and extrapolating the P - V EOS of amorphous nitrogen obtained as described below.

We performed FPMD simulations of amorphous nitrogen—what we expect to be an analog of η -N—by quenching the high-density liquid to lower temperatures. The structural analysis of the FPMD trajectories show that the resulting phase is composed of a mixture of both 2- and 3-coordinated atoms, consistent with previous experimental work³ suggesting that η -N has an average coordination of 2.5(3). There have been several measurements of the band gap of η -N characterizing it as a narrow gap semi-conductor with reported values for the gap near 0.6 eV above 150 GPa.³⁻⁵ The band gap was found to decrease upon further compression, with an extrapolation that suggests metallization at pressures near 300 GPa,⁵ well above the GH metallization estimate for atomic nitrogen but below that for molecular N. We have computed the DOS of amorphous nitrogen over the range of pressures from 90 to 330 GPa. Within PBE, although we find a substantial decrease in electronic states at the Fermi level, our calculations do not show a band gap opening for any of the pressures

considered. This is not surprising, as Peierls distortions can be easily missed or largely underestimated with DFT.³⁶ When we perform structural relaxations on the quenched liquid configurations and then compute the band gap using PBE0 (25% HF exchange), we find a gap, which persists even above 300 GPa. Clearly, if one wishes to apply hybrid techniques to calculate the electronic properties of η -N accurately, the appropriate mixture of HF exchange must be determined. One way to calibrate the hybrid functionals is by comparing with quantum Monte Carlo calculations, which will be subject of a follow-up article.⁴¹

IV. CONCLUSIONS

We have analyzed the electronic and structural properties of liquid nitrogen over a wide pressure and temperature range and show that the metallic behavior in the polymeric and atomic liquids is strongly correlated with the amount of 2-coordinated atoms present. The computed DC conductivity of these liquids is approximately $3000 (\Omega\cdot\text{cm})^{-1}$. The presence of chainlike N formations, short lived at high temperature, is what is responsible for the conducting behavior. Our results provide routes for experimental identification of the polymeric liquid through conductivity and reflectivity measurements. This may be particularly useful in the determination of the high-pressure melting curve of nitrogen. Furthermore, we argue that amorphous solid N is the structural and electronic analog of the polymeric liquid. Its semiconducting behavior can be understood in terms of a Peierls distortion of the N chains. Further analysis of this phase will be reported in a follow-up paper.

ACKNOWLEDGMENTS

This work was performed under the auspices of the US Department of Energy (DOE) at the University of California/LLNL under Contract No. DE-AC52-07NA27344. The authors acknowledge support from NSERC, Killam Trusts, CFI, and Acenet. We thank Sebastien Hamel for useful discussions.

¹M. Eremets, A. Gavriluk, I. Trojan, D. Dzivenko, and R. Boehler, *Nature Mater.* **3**, 558 (2004).

²V. Iota, C. S. Yoo, and H. Cynn, *Science* **283**, 1510 (1999).

³A. F. Goncharov, E. Gregoryanz, H. K. Mao, Z. Liu, and R. J. Hemley, *Phys. Rev. Lett.* **85**, 1262 (2000).

⁴M. I. Eremets, R. J. Hemley, H. K. Mao, and E. Gregoryanz, *Nature (London)* **411**, 170 (2001).

⁵E. Gregoryanz, A. F. Goncharov, R. J. Hemley, and H. K. Mao, *Phys. Rev. B* **64**, 052103 (2001).

⁶M. J. Lipp, J. P. Klepeis, B. J. Baer, H. Cynn, W. J. Evans, V. Iota, and C. S. Yoo, *Phys. Rev. B* **76**, 014113 (2007).

⁷C. Mailhot, L. H. Yang, and A. K. McMahan, *Phys. Rev. B* **46**, 14419 (1992).

⁸M. M. G. Alemany and J. L. Martins, *Phys. Rev. B* **68**, 024110 (2003).

⁹W. D. Mattson, D. Sanchez-Portal, S. Chiesa, and R. M. Martin, *Phys. Rev. Lett.* **93**, 125501 (2004).

¹⁰F. Zahariev, A. Hu, J. Hooper, F. Zhang, and T. Woo, *Phys. Rev. B* **72**, 214108 (2005).

¹¹H. L. Yu, G. W. Yang, X. H. Yan, Y. Xiao, Y. L. Mao, Y. R. Yang, and M. X. Cheng, *Phys. Rev. B* **73**, 012101 (2006).

¹²X. Wang, Z. He, Y. M. Ma, T. Cui, Z. M. Liu, B. Liu, J. F. Li, and G. T. Zou, *J. Phys. Condens. Matter* **19**, 425226 (2007).

¹³Y. Yao, J. S. Tse, and K. Tanaka, *Phys. Rev. B* **77**, 052103 (2008).

¹⁴J. Kotakoski and K. Albe, *Phys. Rev. B* **77**, 144109 (2008).

¹⁵C. J. Pickard and R. J. Needs, *Phys. Rev. Lett.* **102**, 125702 (2009).

¹⁶Y. Ma, A. R. Oganov, Z. Li, Y. Xie, and J. Kotakoski, *Phys. Rev. Lett.* **102**, 065501 (2009).

¹⁷X. Wang, F. Tian, L. Wang, T. Cui, B. Liu, and G. Zou, *J. Chem. Phys.* **132**, 024502 (2010).

¹⁸W. J. Nellis, N. C. Holmes, A. C. Mitchell, and M. van Thiel, *Phys. Rev. Lett.* **53**, 1661 (1984).

¹⁹H. B. Radousky, W. J. Nellis, M. Ross, D. C. Hamilton, and A. C. Mitchell, *Phys. Rev. Lett.* **57**, 2419 (1986).

- ²⁰W. J. Nellis, H. B. Radousky, D. C. Hamilton, A. C. Mitchell, N. C. Holmes, K. B. Christianson, and M. van Thiel, *J. Chem. Phys.* **94**, 2244 (1991).
- ²¹S. Mazevet, J. D. Johnson, J. D. Kress, L. A. Collins, and P. Blottiau, *Phys. Rev. B* **65**, 014204 (2001).
- ²²S. Mazevet, J. D. Kress, L. A. Collins, and P. Blottiau, *Phys. Rev. B* **67**, 054201 (2003).
- ²³B. Boates and S. A. Bonev, *Phys. Rev. Lett.* **102**, 015701 (2009).
- ²⁴D. Donadio, L. Spanu, I. Duchemin, F. Gygi, and G. Galli, *Phys. Rev. B* **82**, 020102 (2010).
- ²⁵W. Kohn and L. Sham, *Phys. Rev.* **140**, A1133 (1965).
- ²⁶J. P. Perdew, K. Burke, and M. Ernzerhof, *Phys. Rev. Lett.* **77**, 3865 (1996).
- ²⁷G. Kresse and J. Hafner, *Phys. Rev. B* **47**, 558 (1993); *Comput. Mater. Sci.* **6**, 15 (1996).
- ²⁸M. I. Eremets, A. G. Gavriiliuk, N. R. Serebryanaya, I. A. Trojan, D. A. Dzivenko, R. Boehler, H. K. Mao, and R. J. Hemley, *J. Chem. Phys.* **121**, 11296 (2004).
- ²⁹E. Gregoryanz, A. F. Goncharov, C. Sanloup, M. Somayazulu, H. K. Mao, and R. J. Hemley, *J. Chem. Phys.* **126**, 184505 (2007).
- ³⁰A. F. Goncharov and J. C. Crowhurst, *Phys. Rev. Lett.* **96**, 055504 (2006).
- ³¹X. Gonze, J. M. Beuken, R. Caracas, F. Detraux, M. Fuchs, G. M. Riganese, L. Sindic, M. Verstraete, G. Zerah, F. Jollet, M. Torrent, A. Roy, M. Mikami, P. Ghosez, J. Y. Raty, and D. C. Allan, *Comput. Mater. Sci.* **25**, 478 (2002).
- ³²X. Gonze, G. M. Riganese, M. Verstraete, J. M. Beuken, Y. Pouillon, R. Caracas, F. Jollet, M. Torrent, G. Zerah, M. Mikami, P. Ghosez, M. Veithen, J.Y. Raty, V. Olevano, F. Bruneval, L. Reining, R. Godby, G. Onida, D. R. Hamann, and D. C. Allan, *Z. Kristallogr.* **220**, 558 (2005).
- ³³B. Holst, R. Redmer, and M. P. Desjarlais, *Phys. Rev. B* **77**, 184201 (2008).
- ³⁴D. A. Horner, J. D. Kress, and L. A. Collins, *Phys. Rev. B* **77**, 064102 (2008).
- ³⁵A. J. Heeger, *Rev. Mod. Phys.* **73**, 681 (2001).
- ³⁶M. Kertesz, C. H. Choi, and S. Yang, *Chem. Rev.* **105**, 3448 (2005).
- ³⁷D. Jiang, X. Q. Chen, W. Luo, and W. A. Shelton, *Chem. Phys. Lett.* **483**, 120 (2009).
- ³⁸J. P. Perdew, M. Ernzerhof, and K. Burke, *J. Chem. Phys.* **105**, 9982 (1996).
- ³⁹A. Pohl, H. Meider, and M. Springborg, *J. Mol. Struct.* **305**, 165 (1994).
- ⁴⁰P. P. Edwards and M. J. Sienko, *Acc. Chem. Res.* **15**, 87 (1982).
- ⁴¹B. Boates and S. A. Bonev (unpublished).